



Research article

Identification of anoikis-related subtypes and development of risk stratification system in skin cutaneous melanoma

Jun Tian^{a,1}, Zi-jian Cao^{b,1}, Yuan Zhang^c, Jin-ke Zhou^b, Li Yang^{a,*}^a Department of Dermatology, Shaanxi Provincial People's Hospital, Xi'an, 710068, China^b Department of Dermatology, The 63600 Hospital of PLA, Lanzhou, 732750, China^c Department of Oncology, Shaanxi Provincial People's Hospital, Xi'an 710068, China

ARTICLE INFO

Keywords:Skin cutaneous melanoma
Anoikis
Prognosis
Immunotherapy
Tumor microenvironment

ABSTRACT

Background: Anoikis, a form of apoptosis induced by cell detachment, plays a key role in cancer metastasis. However, the potential roles of anoikis-related genes (ARGs) in assessing the prognosis of skin cutaneous melanoma (SKCM) and the tumor microenvironment (TME) remain unclear.

Methods: The data from TCGA corresponding to transcriptomic expression patterns for patients with SKCM were downloaded and utilized to screen distinct molecular subtypes by a non-negative matrix factorization algorithm. The prognostic signature was constructed by least absolute shrinkage and selection operator (LASSO) Cox regression and was validated in SKCM patients from the GEO cohort. Moreover, the relationship of the ARG_score with prognosis, tumor-infiltrating immune cells, gene mutation, microsatellite instability (MSI), and immunotherapy efficacy.

Results: We screened 100 anoikis-related differentially expressed genes between SKCM tissues and normal skin tissues, which could divide all patients into three different subtypes with significantly distinct prognosis and immune cell infiltration. Then, an anoikis-related signature was developed based on subtype-related DEGs, which could classify all SKCM patients into low and high ARG_score groups with differing overall survival (OS) rates. ARG_score was confirmed to be a strong independent prognostic indicator for SKCM patients. By combining ARG_score with clinicopathological features, a nomogram was constructed, which could accurately predict the individual OS of patients with SKCM. Moreover, low ARG_score patients presented with higher levels of immune cell infiltration, TME score, higher tumor mutation burden, and better immunotherapy responses.

Conclusions: Our comprehensive analysis of ARGs in SKCM provides important insights into the immunological microenvironment within the tumor of SKCM patients and helps to forecast prognosis and the response to immunotherapy in SKCM patients, thereby making it easier to tailor more effective treatment strategies to individual patients.

* Corresponding author.

E-mail address: ledou2013baby@qq.com (L. Yang).¹ Authors contributed equally to this work.<https://doi.org/10.1016/j.heliyon.2023.e16153>

Received 19 October 2022; Received in revised form 2 May 2023; Accepted 7 May 2023

Available online 9 May 2023

2405-8440/© 2023 The Authors. Published by Elsevier Ltd. This is an open access article under the CC BY-NC-ND license (<http://creativecommons.org/licenses/by-nc-nd/4.0/>).

1. Introduction

Skin cutaneous melanoma (SKCM) is the most aggressive type of skin cancer that originates from melanocytes [1]. It is most prevalent in the head and neck [2]. The incidence and morbidity of SKCM have risen in recent years [3,4]. Its development involves a complex interaction between environmental factors, mainly sunlight exposure, and genetic alterations [1]. Patients with early-stage disease can be cured by surgery, in many cases, tumors are only detected when they are more advanced at which time patients exhibit a markedly poorer prognosis [5]. Because metastatic melanoma is not sensitive to conventional radiotherapy or chemotherapy [6], the treatment of melanoma remains a great challenge.

Normal adherent cells need to be anchored to an extracellular matrix (ECM) substrate in order to survive and proliferate, and when a cell loses contact with its ECM or neighboring cells, cells undergo a specific type of apoptosis called anoikis [7]. This cell death is based on the loss of cell-matrix interactions mediated by intrinsic and extrinsic apoptotic pathways [8]. Anoikis is a key cellular program, and this process can be viewed as a critical event in ensuring normal development and tissue homeostasis [9]. Anoikis acts as an important defense for the organism by preventing exfoliated cells from re-adhering to new substrates in incorrect locations and their stunted growth [9]. However, cancer cells can survive in suspension without ECM adhesion or proliferate at ectopic sites where ECM proteins differ from their original counterparts, leading to greater metastatic potential and drug resistance [7,9]. This lack of anoikis is becoming a hallmark of cancer cells and contributes to the formation of metastases in distant organs [7]. Several anoikis-related genes (ARGs) have been reported to play central roles in cancer initiation and progression, including ovarian cancer, gastric cancer, and lung cancer [10–13]. Takeshita et al. [10] revealed that ANGPTL2 repressed peritoneal metastasis of ovarian cancer cells by suppressing anoikis resistance. In gastric cancer, nuclear MYH9 promotes CTNNB1 transcription by binding to the CTNNB1 promoter and interacting with myosin light chain 9, beta-actin, and RNA polymerase II, thereby making gastric cancer cells resistant to anoikis [11]. Takeshita et al. [12] found that the GDH1 promotes anoikis resistance and tumor metastasis through CamKK2-AMPK signaling in LKB1-Deficient lung cancer. However, most of the studies are limited to 1 to 2 ARGs, there are no systematic studies on ARGs in SKCM.

Therefore, in this paper, a comprehensive analysis of anoikis-related genes was performed through the SKCM transcriptomic and genomics sequencing database. Consensus clustering was performed and SKCM were classified into three clusters with remarkably diverse prognosis and immune cell infiltration in the tumor microenvironment (TME). Then, a prognostic signature (ARG_score) was constructed based on the training cohort samples, and its predictive accuracy was validated in an independent testing cohort. We further analyzed the differences between low and high ARG_score groups regarding immune cell infiltration, gene mutation, microsatellite instability (MSI), and immunotherapy efficacy. To increase the clinical utility of this signature, a prognostic nomogram integrating ARG_score and clinical traits was established. In conclusion, our finding suggests that anoikis plays a crucial role in the tumor immune microenvironment (TIME) and in predicting patient clinical outcomes and immunotherapy efficacy.

2. Materials and methods

2.1. Data source

Raw data, composed of transcriptomic matrix and clinical information of SKCM ($n = 471$) and normal tissues ($n = 1$) in fragments per kilobase million (FPKM) format, was obtained from the TCGA database. The expression data of normal skin samples ($n = 812$) within the Genotype-Tissue Expression (GTEx) collection of RNA-seq experiments (platform: Illumina HiSeq 2000) were obtained from the GTEx portal (<https://gtexportal.org/home/>). In addition, the GSE65904 dataset for SKCM ($n = 210$) with available overall survival (OS) time was collected from the public Gene Expression Omnibus (GEO) database. RNA expression profiles in all datasets were transformed into transcripts per million (TPM), with batch effects removed using the “ComBat” algorithm in the “sva” R package [14].

2.2. Identification of differentially expressed ARGs

A total of 468 ARGs from the GeneCards (<https://www.genecards.org/>) were identified with a relevance score >0.4 (Supplementary Table S1). We set $|\log_2$ fold change (FC)| > 1 and false discovery rate (FDR) < 0.05 as a threshold to screen out differentially expressed ARGs through performing the “limma” package in R software.

2.3. Consistent clustering of ARGs

To identify different gene transcriptional regulation patterns, we conducted the non-negative matrix factorization (NMF) cluster analysis based on the expression of differentially expressed ARGs. The consensus clustering algorithm determined the clusters and their stability through the “NMF” R package. Kaplan Meier curves were used to evaluate the OS of different SKCM patients and the log-rank test was used. In addition, we identified the content of tumor-infiltrating immune cells (TIICs) by the CIBERSORT algorithm and compared their differences between different molecular subtypes.

2.4. Establishment and validation of ARG_score

We normalized DEGs extracted from different anoikis clusters and extracted overlapping DEGs. The patients included in the TCGA dataset served as the training cohort, and the patients in the GSE65904 dataset served as the testing cohort. The “survival” package was used to identify the association between gene expression levels and patients’ OS using univariate Cox regression analysis on DEGs of

the training cohort. Thereafter, the least absolute shrinkage and selection operator (LASSO) Cox regression algorithm was performed to establish a prognostic signature (ARG_score), which could screen out DEGs with optimal performance and calculate their coefficients. The ARG_score for each patient will be estimated as:

$ARG_score = \sum expi * coefi$, where *exp* and *coef* are expression levels and correlation coefficients, respectively.

The median ARG_score in the training cohort was used to separate SKCM samples into low and high ARG_score groups, after which this same formula and cutoff were used to assess SKCM patients in the testing cohort. Survival curve of patients in the training and testing cohorts was plotted based on two ARG_score groups. PCA was conducted to reduce the dimensionality, judging the ability to distinguish patients. The receiver operating characteristic (ROC) curves were plotted to evaluate the performance of the model with the “timeROC” R package.

2.5. Establishment and evaluation of a nomogram

We investigated whether ARG_score was an independent predictor of OS using univariate and multivariate independent prognostic analysis. Additionally, stratified survival analysis was conducted to evaluate OS differences between two ARG_score groups based on age, sex, tumor location, stage, Breslow depth, ulceration, and tumor status. To fully expand the predictive performance of ARG_score, we constructed another quantitative method, a nomogram to predict the individual probability of survival based on the independent prognostic factors by using “rms” package in R. The predictive accuracy of the nomogram was evaluated using the ROC curve and calibration curve plot.

2.6. Analysis of tumor immune microenvironment (TIME)

To explore the role of ARG_score in immune cell infiltration, we investigated the distribution of 22 types of TIICs in two ARG_score groups by CIBERSORT algorithm [15]. Moreover, association strengths between the fraction of 22 types of TIICs and ARG-score were further explored utilizing Spearman correlation analysis. In addition, the ESTIMATE algorithm was used to calculate the immune score, and the interstitial score to reflect the microenvironmental status.

2.7. Prediction of immunotherapy response for SKCM

To explore the ARG_score to predict the effect of immunotherapy, we used the TIDE online database (<http://tide.dfci.harvard.edu/>). The immunophenoscore (IPS) of SKCM patients from the TCGA database was downloaded from The Cancer Immunome Atlas (TCIA) [16]. The sensitivity to PD-1 and CTLA4 antibodies of patients with low and high ARG_score was studied by the “ggpubr” R package. Moreover, the association between immune checkpoints and the ARG_score was calculated, and the box plot was plotted by the “reshape2” and “ggplot2” R packages.

2.8. Correlation of tumor mutation burden (TMB) and ARG_score

The somatic mutation data of SKCM was obtained from the TCGA database, and the gene mutation type and frequency for every sample were calculated. The “Maftools” R package and its “oncoplot” function were used to present mutational differences between two ARG_score groups. The TMB scores of the two ARG_score groups were compared, and the correlation of the TMB scores with the ARG_score was evaluated. Moreover, the OS difference between low and high TMB groups was compared by the Kaplan-Meier survival analysis. Next, we further evaluated the synergistic effect of TMB and ARG_score groups in prognostic stratification.

2.9. Functional enrichment analysis

To study the biological processes correlated with ARG_score, GO and KEGG analyses were performed by the “clusterProfiler” R package. With the “limma” R package, differential genes ($|\log_2 FC| > 1$ and $FDR < 0.05$) between different ARG_score groups were screened out and applied to GO and KEGG pathway analysis.

2.10. Cell culture and real-time quantitative PCR

Human skin melanocyte cell line (PIG1) and two melanoma cell lines (A375 and SK-MEL-1) were obtained from Shanghai Institute of Cell Biology, Chinese Academy of Sciences. The cell lines were cultured in Dulbecco’s modified Eagle’s medium (Gibco) supplemented with 10% fetal bovine serum (FBS; Gibco), 100 U/ml penicillin, and 100 mg/ml streptomycin (Invitrogen) and incubated at 37 °C with 5% CO₂. Total RNA was extracted from cells using Trizol (Invitrogen). The PrimeScript RT Master Mix (Takara, Japan) was used to reverse-transcribe RNA into complementary DNA (cDNA). Following the manufacturer’s instructions, RT-qPCR was conducted using SYBR Green PCR Kit (TaKaRa, Japan).

2.11. Verification of the protein expression of signature genes

The protein expression levels of the signature genes in normal skin and melanoma tissues were verified using the immunohistochemical data obtained from The Human Protein Atlas (<https://www.proteinatlas.org/>).

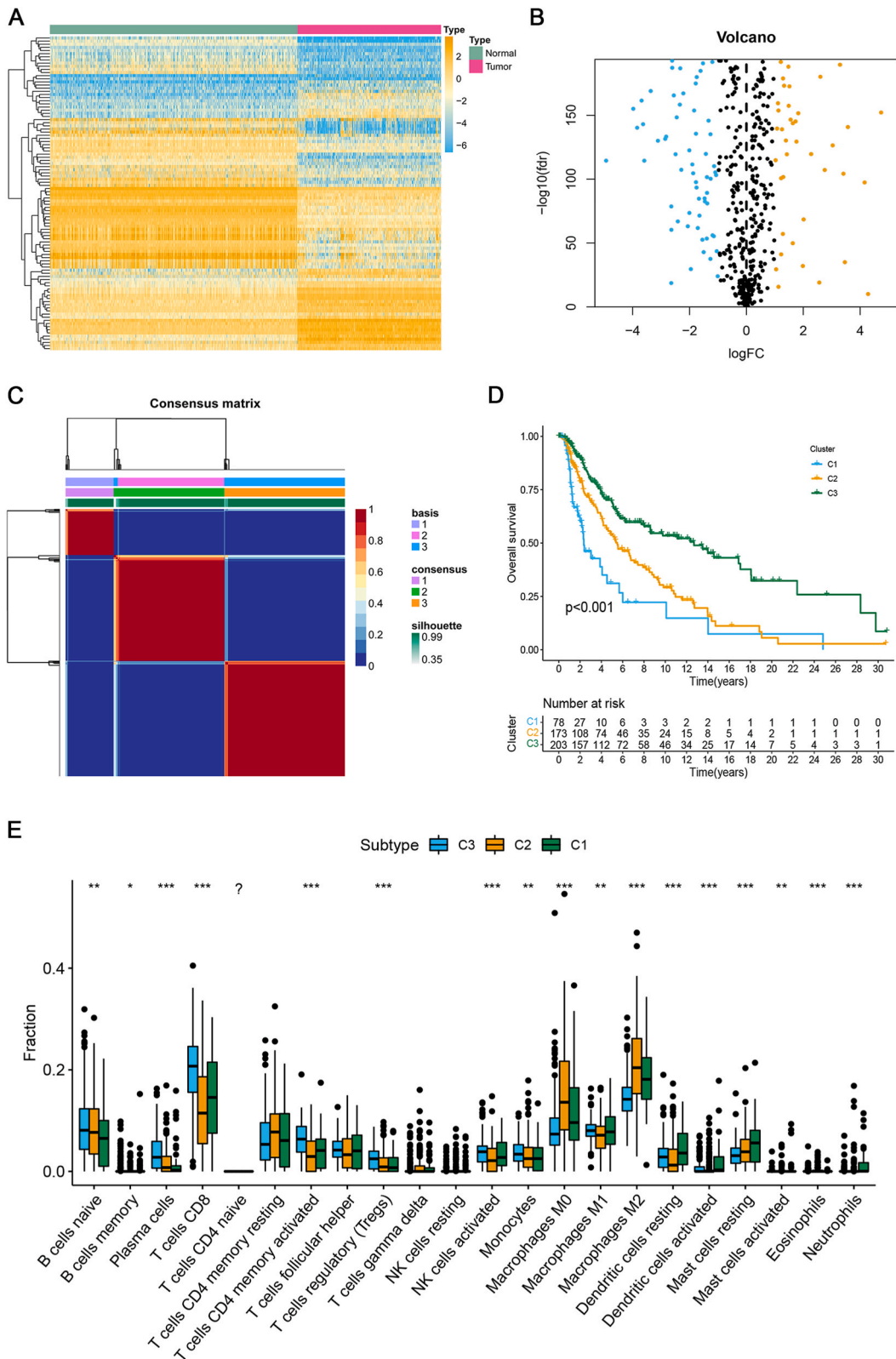


Fig. 1. Anoiis-related genes classify the clinical and molecular features of SKCM. (A) The heatmap of the expression profiles of differentially expressed ARGs between the tumor samples and normal samples. (B) Volcano plot of differentially expressed ARGs. (C) NMF consensus clustering for the k value was 3. (D) Kaplan-Meier for SKCM patients in three clusters. (E) The distribution of infiltrating immune cells in three distinct clusters.

3. Results

3.1. Identification of anoikis-related subtypes in SKCM

The study workflow is shown in [Supplementary Fig. 1](#). In total, 813 normal skin samples and 471 SKCM samples were obtained from TCGA and GTEx databases. Then, a total of 100 differentially expressed ARGs were acquired, including 39 upregulated ARGs and 61 down-regulated ARGs ([Fig. 1A](#) and [B](#)). To further explore the expression characteristics of 100 anoikis-related DEGs in SKCM, the NMF clustering analysis was performed which suggested that the training cohort could be well divided into three clusters, namely C1, C2, and C3, respectively ([Fig. 1C](#)). Kaplan-Meier survival curves revealed clear differences in OS among the three clusters, among which cluster C3 had significantly longer OS than the other two clusters ([Fig. 1D](#)). Furthermore, we used the CIBERSORT algorithm to

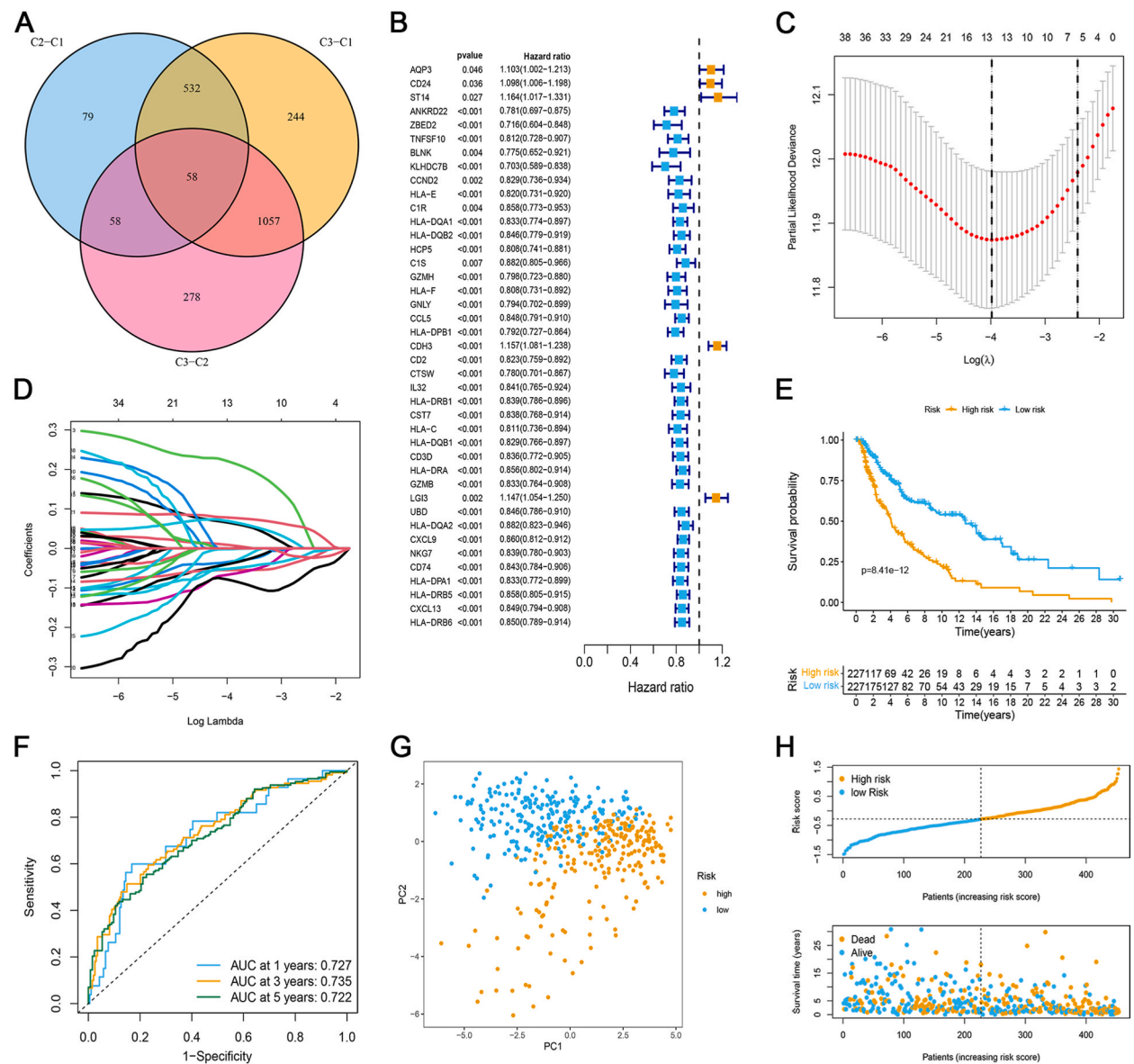


Fig. 2. Establishment and evaluation of the ARG_score in the training cohort. (A) The overlapping DEGs of three anoikis clusters. (B) Forest plot of 41 DEGs associated with OS. (C) The number that corresponded to the point with the smallest cross-verification error was the gene numbers included in the LASSO regression risk model. (D) The lines of different colors represent the trajectory of the correlation coefficient of different factors in the model with the increase of Log Lamda. (E) Kaplan-Meier curve to show OS of patients in different ARG_score groups. (F) Prediction of the sensitivity and specificity of 1-, 3-, and 5- years survival in ROC curves based on the ARG_score. (G) PCA of the training cohort. (H) Survival status of SKCM patients and the distribution plot of ARG_score. (For interpretation of the references to color in this figure legend, the reader is referred to the Web version of this article.)

estimate the quantification of different cell infiltration in SKCM TME. Surprisingly, cluster C3 is characterized by increased immune cell infiltration, while cluster C2 is characterized by immunosuppression. Specifically, cluster C3 had higher infiltration levels of activated memory CD4⁺ T cells, CD8⁺ T cells, activated NK cells, M1 macrophages, and dendritic cells, while cluster C2 is very abundant in M0 macrophages, M2 macrophages, and resident memory CD4⁺ T cells (Fig. 1E).

3.2. Establishment and evaluation of the ARG_score

According to the cut-off thresholds of $|FC| > 1.5$ and $FDR < 0.05$, we discovered 58 DEGs associated with the anoikis phenotype (Fig. 2A). To determine the correlation between DEGs and OS of SKCM patients, a univariate Cox regression analysis was performed in the training cohort. Consequently, 41 DEGs were found to be associated with OS (Fig. 2B). After using the LASSO regression method, 13 DEGs were selected to develop a prognostic signature, namely ARG_score (Fig. 2C and D). The ARG_score was assigned to each patient in the training cohort using the LASSO coefficient combination of the expression level of the 13 DEGs. The LASSO coefficient of the 13 DEGs is listed in Supplementary Table S2. Using the median ARG_score as a cutoff value, SKCM samples were partitioned into low and high ARG_score groups. Patients in the low ARG_score group demonstrated a substantial survival benefit compared to the high ARG_score group (Fig. 2E). The AUC values for one, three, and five years were 0.727, 0.735, and 0.722, respectively (Fig. 2F). Patients in the high ARG_score group could be completely distinguished from those in the low ARG_score group using principal component analysis (PCA) (Fig. 2G). Furthermore, the distribution plot of ARG_score and survival status demonstrated that as the ARG_score increased, more patients died (Fig. 2H).

To further test the robustness of the ARG_score, the same coefficient and formula was used to calculate the ARG_score in the GSE65904 testing cohort. Similarly, patients with high ARG_score had poorer OS (Fig. 3A). The AUC values at one, three, and five years confirmed that the ARG_score had a well-prediction performance (Fig. 3B). PCA analysis demonstrated a reliable clustering ability of ARG_score (Fig. 3C). Additionally, the distribution plot of ARG_score and survival status demonstrated that as the ARG_score increased, more patients died (Fig. 3D).

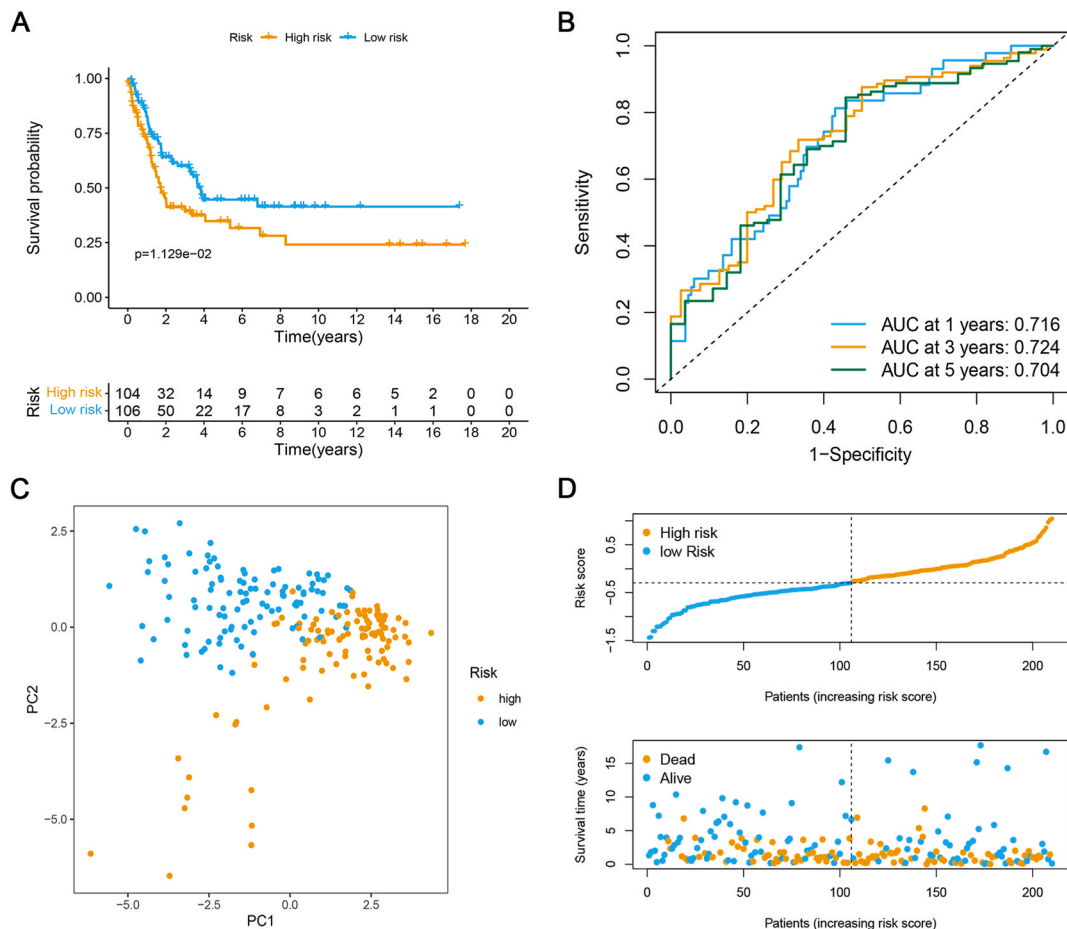


Fig. 3. Validation of the ARG_score in the testing cohort. (A) Kaplan-Meier curve to show OS of patients in different ARG_score groups. (B) Prediction of the sensitivity and specificity of 1-, 3-, and 5- years survival in ROC curves based on the ARG_score. (C) PCA of the testing cohort. (D) Survival status of SKCM patients and the distribution plot of ARG_score.

3.3. Development and evaluation of a prognostic nomogram

The prognostic value of clinical features and ARG_score in the training cohort was further studied by univariate analysis. The results demonstrated that age, TNM stage, and ARG_score were significantly correlated with OS (Fig. 4A), which were further confirmed by multivariate Cox regression analysis as independent prognostic indicators (Fig. 4B). Moreover, we discovered that the ARG_score had greater survival discriminating value in several clinical subgroups, including various age groups, sex groups, Breslow depth groups, TNM stage groups, ulceration groups, and tumor status groups (Supplementary Fig. 2A–M). The ARG_score also has a good prognostic value in patients with different tumor locations, especially primary tumors, regional cutaneous, and regional lymph nodes (Supplementary Fig. 2N–P). The nomogram comprising clinical traits and ARG_score was fabricated (Fig. 4C), which showed robust accuracy in predicting OS at one, three, and five years (AUC = 0.796, 0.779, and 0.751, respectively) (Fig. 4D). Moreover, the calibration curves revealed that actual survival was close to predicted survival (Fig. 4E).

3.4. Indicative role of ARG_score in TIME

To comprehensively explore the role ARG_score in the TIME, we explored the relationship between different ARG_score groups and the immune landscape, including TIICs and TME scores. In terms of TIICs, a higher fraction of activated memory CD4⁺ T cells, CD8⁺ T cells, activated NK cells, and M1 macrophages, and plasma cells were observed in the low ARG_score group, while the proportion of M0

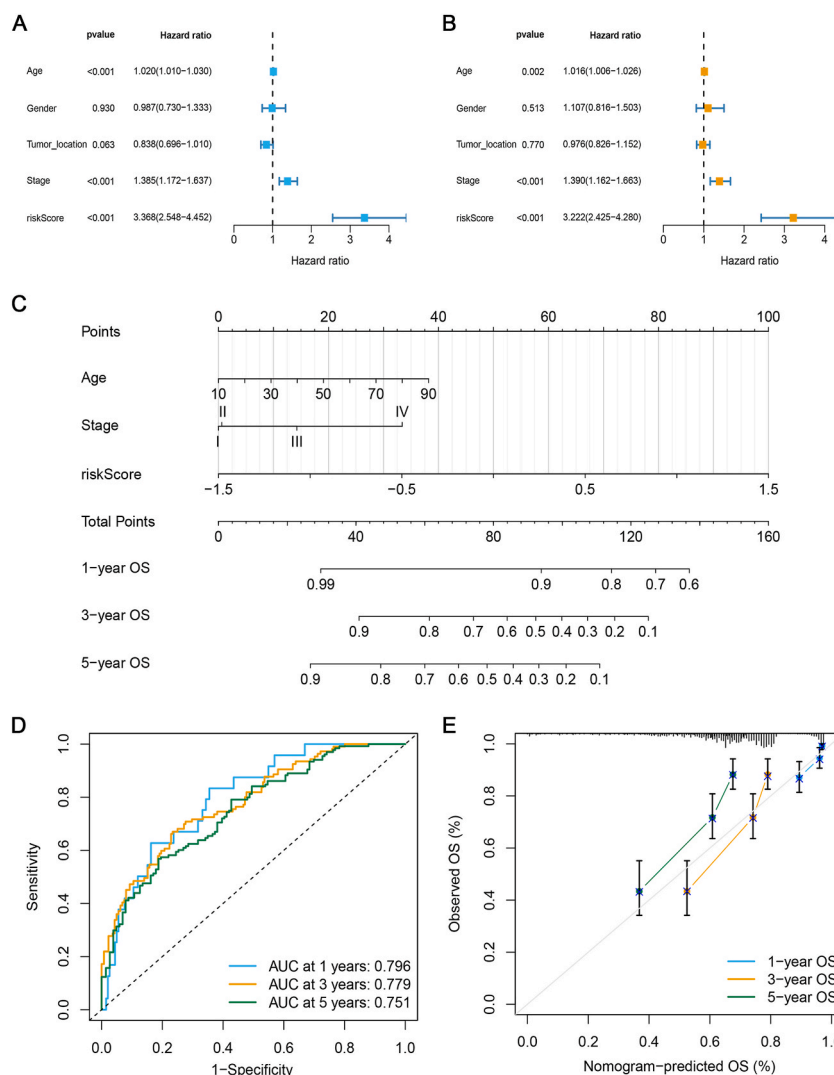


Fig. 4. The nomogram predicting OS of SKCM patients. (A, B) Univariate and multivariate Cox regression analyses between ARG_score and OS. (C) Nomogram based on ARG_score, age, and stage. (D) The ROC curves of the nomogram in predicting 1-, 3-, and 5-year OS. (E) The calibration curves show the concordance between the predicted survival and actual survival.

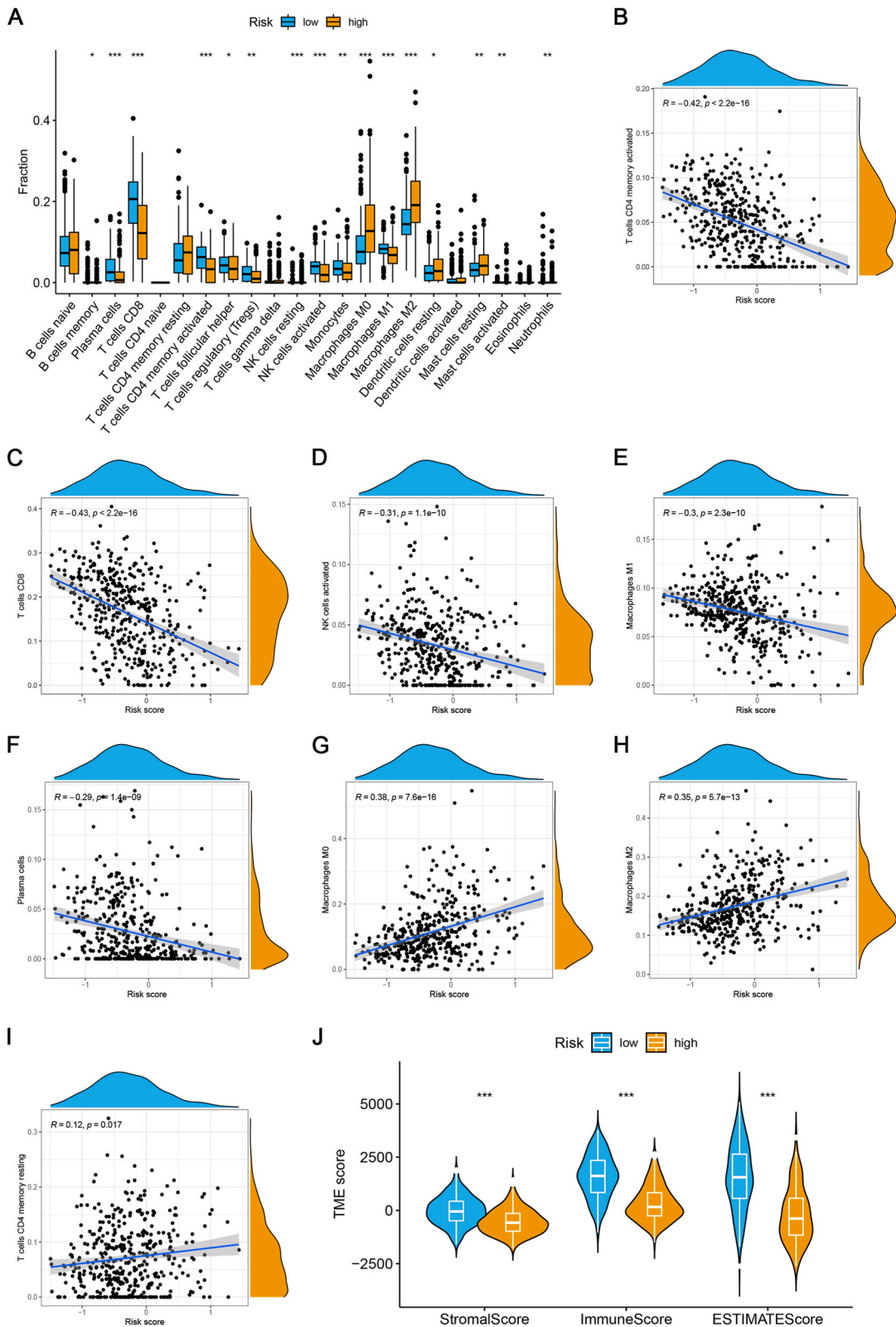


Fig. 5. The relationship between ARG score and TIME. (A) The correlation of ARG_score with 22 types of TIICs. (B–I) The infiltrating levels of different immune cells in the high and low ARG_score groups. (J) The distribution of immune, stromal, and ESTIMATE scores in high and low ARG_score groups.

macrophages, M2 macrophages, and resting memory CD4⁺ T were lower in low ARG score group (Fig. 5A). Similarly, the ARG_score had evident negative associations with abundance of activated memory CD4⁺ T cells, CD8⁺ T cells, activated NK cells, M1 macrophages, and plasma cells (Fig. 5B–F), and had evident positive associations with fraction of resting M0 macrophages, M2 macrophages, and resting memory CD4⁺ T (Figure G–I). In terms of TME scores, the ESTIMATE, stromal, and immune scores of the low ARG_score groups were evidently higher than those in the high ARG_score groups (Fig. 5J).

3.5. Mutation landscape between different ARG_score groups

Given that TMB is clinically significant in directing immunotherapy in SKCM patients, we sought to explore the intrinsic correlation between TMB and ARG_score. The low ARG_score group was found to have significantly higher TMB scores (Fig. 6A) and a negative correlation was observed between them (Fig. 6B). Kaplan-Meier analysis demonstrated that the low-TMB group represented a worse OS (Fig. 6C). Dividing SKCM patients into four subgroups according to ARG score and TMB, we found that the prognostic value of ARG_score was not affected by TMB status (Fig. 6D). In addition, the waterfall plot in Fig. 6E and F revealed the differences in the genetic mutations between the high (88.94%) and low ARG_score groups (93.75%) in the training cohort. TTN was the most widely mutated gene in both groups, while the high ARG_score group had a TTN mutation rate of 68% (Fig. 6E), while the TTN mutation rate in the low ARG_score group was 75% (Fig. 6F).

3.6. The role of ARG_score in immunotherapy

Previous results suggest that ARG_score can influence immune cell infiltration. Therefore, we compared responses to immunotherapy in patients with high and low ARG scores. Our results demonstrated that patients with high ARG_score have a higher levels of TIDE scores, which indicates that the low ARG_score patients were more sensitive to immunotherapy compared to the high ARG_score patients (Fig. 7A) ($P < 0.05$). Whether treated with PD-1 antibody alone or in combination with CTLA-antibody, patients with low ARG_score received higher IPS scores than those with high ARG_score (Fig. 7B–E). In addition, the association of 45 common immune checkpoints with the ARG_score of the training cohort was investigated, of which the expression of 42 immune checkpoints was significantly upregulated in the low ARG_score group, including CTLA4, PD-1, PD-L1 (Fig. 7F).

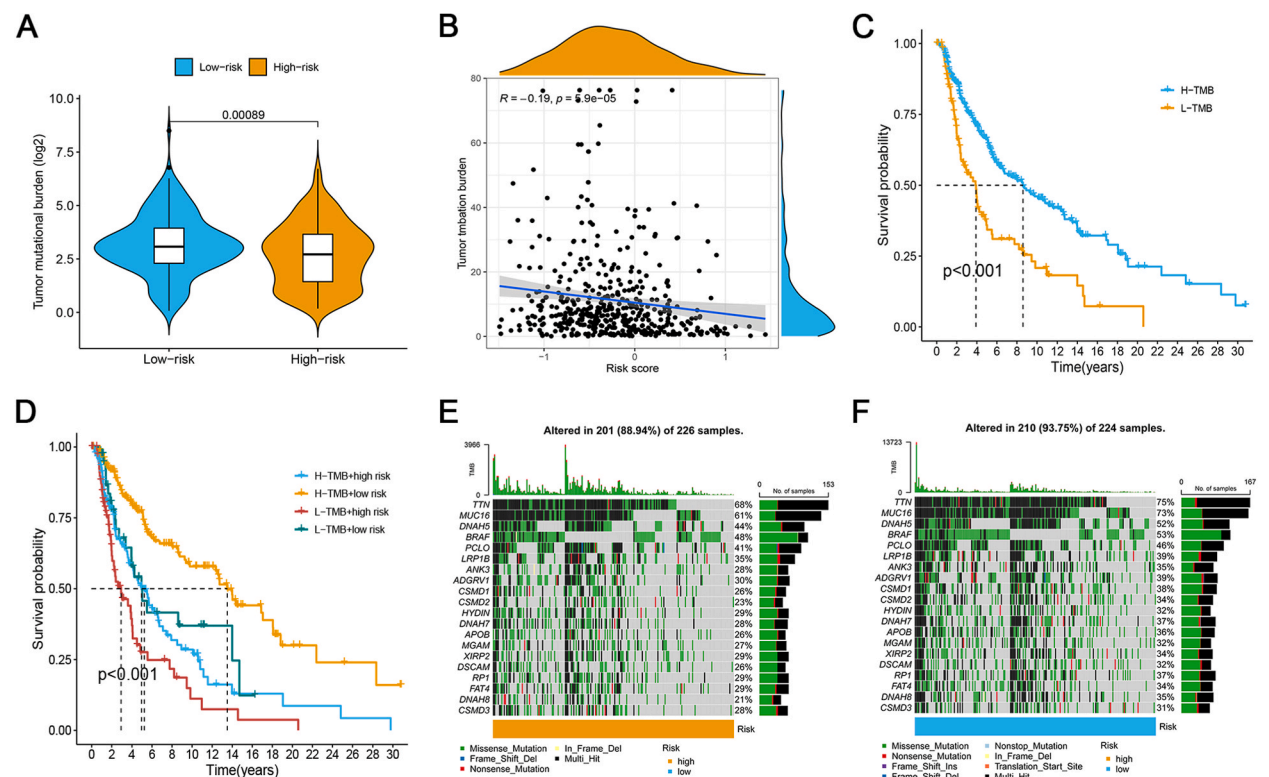


Fig. 6. Mutation landscape between the two ARG_score groups. (A) The differences in the TMB with high and low ARG_score groups. (B) The relationship between ARG_score and TMB. (C) Kaplan-Meier survival analysis of OS in high and low TMB groups. (D) Kaplan-Meier curve to show OS of patients in different TMB and ARG_score groups. (E–F) Mutation rates and types of top 20 genes in the two ARG_score groups.

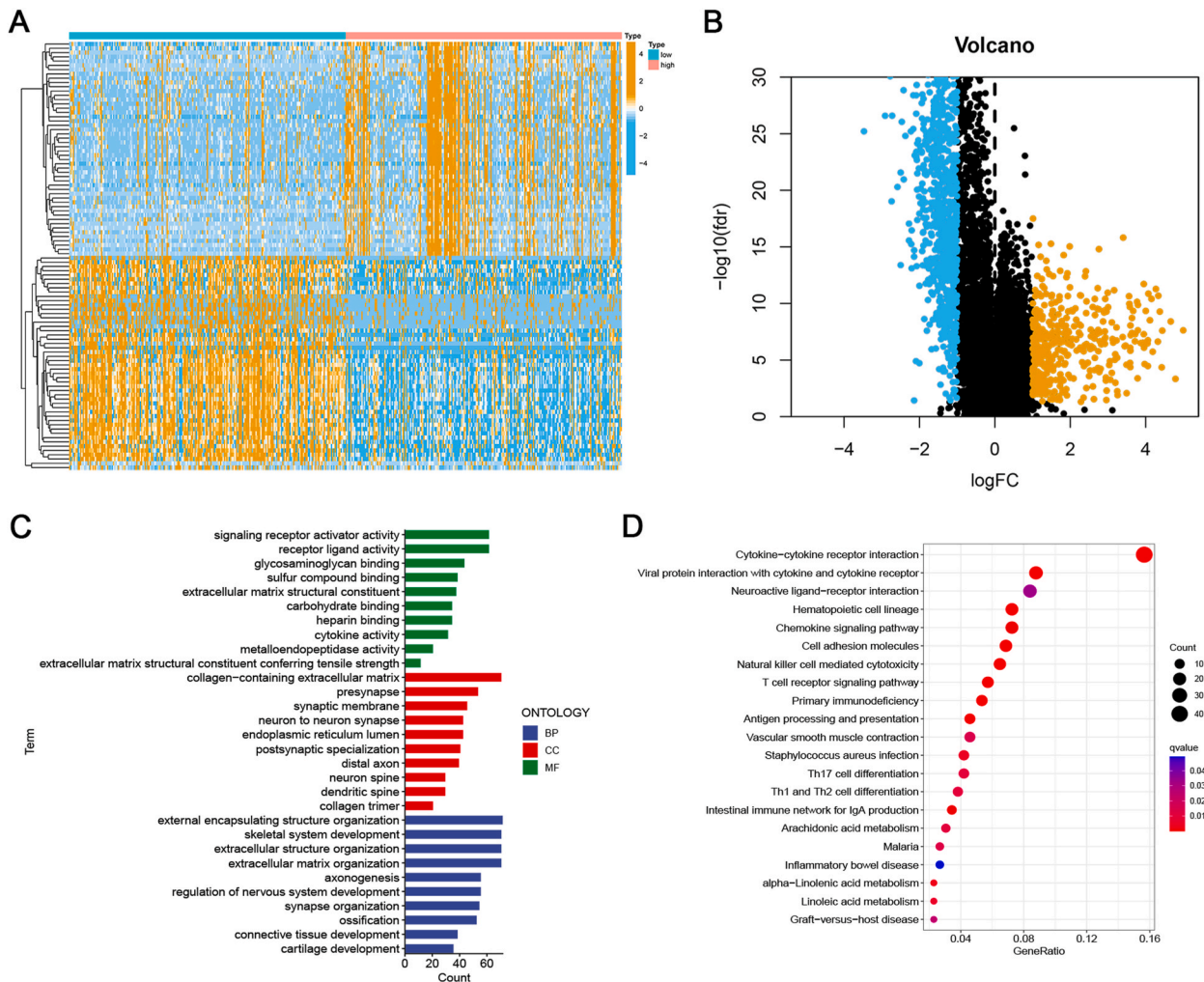


Fig. 8. Functional enrichment analysis of DEGs. (A) The heatmap of the expression profiles of DEGs between the two ARG_socre groups. (B) Volcano plot of DEGs. The orange dots indicate upregulated genes, the blue dots indicate downregulated genes, and the black dots indicate no significant genes. (C) The bar plot of GO analysis in DEGs. (D) The bubble plot of KEGG pathways analysis in DEGs. (For interpretation of the references to color in this figure legend, the reader is referred to the Web version of this article.)

4. Discussion

Anoikis is a type of programmed cell death that is essential for tissue homeostasis and development. However, abnormal execution of anoikis may represent a hallmark of cancer cells. Tumor cells often acquire anoikis resistance, which allows them to begin moving away from the primary lesion, thereby contributing to tumor invasion and migration, the formation of distant organ metastases, and the development of drug resistance [17–20]. Studies have shown that multiple pathways can lead tumor cells to acquire anoikis resistance [9,21–23], which highlights the concept of targeting ARGs to overcome SKCM progression and metastasis. However, there is currently a lack of systematic studies on the role of ARGs in the TME and the prognosis of SKCM.

This study distinguished three distinct subtypes based on anoikis-related DEGs between SKCM samples and normal skin samples. Kaplan-Meier survival curves revealed that patients with cluster C3 had a favorable survival probability than the other two clusters. The characteristics of TME were quite different between the three clusters. Tumors were classified into three immunophenotypes: immunological-inflammatory, immune-desert, and immune-excluded based on the immune background of the tumor [24]. Cluster C3 is characterized by increased immune cell infiltration in TME, including CD4⁺ T cells, CD8⁺ T cells, dendritic cells, and M1 macrophages. The levels of these immune cells directly affect the onset of the adaptive immune response and correlate with a patient survival advantage [25–27]. The infiltration of these immune cells was lowest in cluster C2, and their level in cluster C1 was moderate. There is a tendency to classify Cluster C3 as an immune-inflammatory phenotype, and clusters C1 and C2 into immune-desert phenotype and immune-excluded phenotype, respectively.

We further investigated the DEGs associated with the anoikis phenotype and established a prognostic scoring system in the training cohort to better assess the heterogeneity of individual anoikis patterns. No matter for the training cohort or testing cohort, the

signature of ARGs showed robust ability to predict OS in SKCM patients. The predictive accuracy of the signature was internally and externally validated. In the multivariable Cox analysis, the ARG_score was proven to be a prognostic scoring system independent of other essential clinical features. Subsequently, we established a nomogram comprising ARG_score and clinical characteristics, and it had the latent force to be used as a quantitative tool to predict OS in SKCM patients, which had particular importance in clinical practice.

Melanoma is a highly immunogenic tumor with crosstalk with immune cells in the TME [28,29]. Many immune cell types in the TIME significantly affect the prognosis of patients with SKCM [30]. Hence, we analyzed the relationship between ARG_score and immune landscape, including infiltrating immune cells and TME scores. We found that the ARG_score had significant negative correlations with immune-activating cells, including activated memory CD4⁺ T cells, CD8⁺ T cells, activated NK cells, and M1 macrophages. On the contrary, the ARG_score had significant positive correlations with immune suppressive cells, such as M2 macrophages. Studies have confirmed the presence of tumor-infiltrating lymphocytes (TILs) is generally a positive prognostic indicator for SKCM [30, 31]. The numbers, localization, and phenotypes of TILs can predict the efficacy of immunotherapy in SKCM [32–34]. CD8⁺ T cells play a central role in the adaptive immune response to cancer [35]. CD8⁺ T cell levels in primary SKCM tumors are associated with increased survival [36]. In metastatic melanoma, a high density of CD8⁺ T cells was also reported to be positively correlated with survival [37]. In addition, we also investigated the potential relationship between ARG_score and TME score and found lower stromal and immune scores in the high ARG_score group. This suggests that different ARG_score can have a huge impact on TME shaping.

Anti-PD1/L1 antibodies have become a standard treatment for advanced melanoma and can effectively improve the prognosis by increasing infiltrating CD8⁺ T cells [38–40]. However, only a minority of patients have benefited from immunotherapy. Hence, we sought to assess whether the ARG_score could serve as a novel biomarker to predict patient responses to immunotherapy. We observed that high ARG_score patients had higher TIDE scores, suggesting that patients are more prone to immune escape. We further found that patients with low ARG_score had higher IPS scores than those with high ARG_score, whether treated with PD-1 antibody alone or in combination with CTLA antibody. In addition, the analysis of ICIs showed that most ICIs, such as CTLA4, PD-1, and PD-L1, were significantly upregulated in the low ARG_score group. TMB reflects the level of cancer mutation and the ability to produce neoantigen by malignancies [41]. The lower the TMB, the less likely that T cells will recognize and eradicate tumor antigens [41]. Our results showed higher TMB in the low ARG_score group, suggesting that patients are more likely to benefit from immunotherapy. Dividing SKCM patients into four subgroups according to ARG_score and TMB, we found that the prognostic value of ARG_score was not affected by TMB status. These results demonstrated that ARG_score may serve as a tool to screen SKCM patients suitable for immunotherapy.

However, there were some shortcomings in our study. Firstly, our findings are based on different public databases, and the predictive performance of ARG_score still needed to verify in the large-sample clinical cohort in the future. Secondly, all the findings in this manuscript were of speculation based on the transcriptional analyses using bioinformatics analysis, the exact mechanism of ARGs in SKCM need to be further investigated *in vivo* and *in vitro*. Nonetheless, this work still highlights the importance of TCGA genomic resources that would expand clinicians' understanding of this lethal disease.

5. Conclusions

We performed a comprehensive and systematic analysis of anoikis-related gene expression in SKCM patients and screened three clusters with distinct TME characteristics and prognoses. We further established a prognostic signature that helps predict prognosis and response to immunotherapy in patients with SKCM.

Availability of data and materials

The public datasets were obtained from TCGA (<https://portal.gdc.cancer.gov/>) and GEO (<https://www.ncbi.nlm.nih.gov/geo/>).

Funding

This study was supported by the Natural Science Foundation of Shaanxi Province (No. 2021JQ-919), Shaanxi Provincial People's Hospital 2020 Science Technology Development Incubation foundation (No. 2020YXM-05).

Authors' contributions

JT, and LY conceived and designed the experiments. JT and ZJC performed the experiments. JT and ZJC analyzed and interpreted the data. JT, ZJC, and YZ contributed reagents, materials, analysis tools or data. All authors wrote the paper.

Declaration of competing interest

The authors declare that they have no known competing financial interests or personal relationships that could have appeared to influence the work reported in this paper

Acknowledgements

Not applicable.

Abbreviations

TME	tumor microenvironment
SKCM	skin cutaneous melanoma
LASSO	least absolute shrinkage and selection operator
TIICs	tumor-infiltrating immune cells
MSI	microsatellite instability
DEGs	differentially expressed genes
ECM	extracellular matrix
OS	overall survival
NMF	non-negative matrix factorization
ROC	receiver operating characteristic
TIME	tumor immune microenvironment
IPS	immunophenoscore
KEGG	Kyoto Encyclopedia of Genes and Genomes
GO	Gene Ontology

Appendix A. Supplementary data

Supplementary data to this article can be found online at <https://doi.org/10.1016/j.heliyon.2023.e16153>.

References

- [1] J. Leclerc, R. Ballotti, C. Bertolotto, Pathways from senescence to melanoma: focus on MITF sumoylation, *Oncogene* 36 (48) (2017) 6659–6667, <https://doi.org/10.1038/onc.2017.292>.
- [2] J. Ponto, R.B. Bell, Adjuvant and neoadjuvant therapies in cutaneous melanoma, *Oral Maxillofac. Surg. Clin.* 34 (2) (2022) 315–324, <https://doi.org/10.1016/j.coms.2021.11.010>.
- [3] N. Iglesias-Pena, S. Paradelo, A. Tejera-Vaquerizo, A. Boada, E. Fonseca, Cutaneous melanoma in the elderly: review of a growing problem, *Acta Dermosifiliogr. (Engl. Ed.)* 110 (6) (2019) 434–447, <https://doi.org/10.1016/j.ad.2018.11.009>.
- [4] A. Muntyanu, E. Savin, F.M. Ghazawi, A. Alakel, A. Zubarev, I.V. Litvinov, Geographic variations in cutaneous melanoma distribution in the Russian federation, *Dermatology* 236 (6) (2020) 500–507, <https://doi.org/10.1159/000507617>.
- [5] M.J. Quintanilla-Dieck, C.K. Bichakjian, Management of early-stage melanoma, *Facial Plast. Surg. Clin. North Am.* 27 (1) (2019) 35–42, <https://doi.org/10.1016/j.fsc.2018.08.003>.
- [6] J. Yue, R. Vendramin, F. Liu, O. Lopez, M.G. Valencia, H. Gomes Dos Santos, et al., Targeted chemotherapy overcomes drug resistance in melanoma, *Genes Dev.* 34 (9–10) (2020) 637–649, <https://doi.org/10.1101/gad.333864.119>.
- [7] M. Fujita, M. Sasada, T. Iyoda, R. Nagai, C. Kudo, T. Yamamoto, et al., Anoikis resistance conferred by tenascin-C-derived peptide TNIIIA2 and its disruption by integrin inactivation, *Biochem. Biophys. Res. Commun.* 536 (2021) 14–19, <https://doi.org/10.1016/j.bbrc.2020.12.050>.
- [8] E. Kakavandi, R. Shahbahrami, H. Goudarzi, G. Eslami, E. Faghihloo, Anoikis resistance and oncoviruses, *J. Cell. Biochem.* 119 (3) (2018) 2484–2491, <https://doi.org/10.1002/jcb.26363>.
- [9] P. Paoli, E. Giannoni, P. Chiarugi, Anoikis molecular pathways and its role in cancer progression, *Biochim. Biophys. Acta* 1833 (12) (2013) 3481–3498, <https://doi.org/10.1016/j.bbamcr.2013.06.026>.
- [10] Y. Takeshita, T. Motohara, T. Kadomatsu, T. Doi, K. Obayashi, Y. Oike, et al., Angiopoietin-like protein 2 decreases peritoneal metastasis of ovarian cancer cells by suppressing anoikis resistance, *Biochem. Biophys. Res. Commun.* 561 (2021) 26–32, <https://doi.org/10.1016/j.bbrc.2021.05.008>.
- [11] G. Ye, Q. Yang, X. Lei, X. Zhu, F. Li, J. He, et al., Nuclear MYH9-induced CTNBN1 transcription, targeted by staurosporine, promotes gastric cancer cell anoikis resistance and metastasis, *Theranostics* 10 (17) (2020) 7545–7560, <https://doi.org/10.7150/thno.46001>.
- [12] L. Jin, J. Chun, C. Pan, A. Kumar, G. Zhang, Y. Ha, et al., The PLAG1-GDH1 Axis promotes anoikis resistance and tumor metastasis through CamKK2-AMPK signaling in LKB1-deficient lung cancer, *Mol. Cell* 69 (1) (2018) 87–99.e7, <https://doi.org/10.1016/j.molcel.2017.11.025>.
- [13] H. Zhang, G. Wang, R. Zhou, X. Li, Y. Sun, Y. Li, et al., SPIB promotes anoikis resistance via elevated autolysosomal process in lung cancer cells, *FEBS J.* 287 (21) (2020) 4696–4709, <https://doi.org/10.1111/febs.15272>.
- [14] J.T. Leek, W.E. Johnson, H.S. Parker, A.E. Jaffe, J.D. Storey, The sva package for removing batch effects and other unwanted variation in high-throughput experiments, *Bioinformatics* 28 (6) (2012) 882–883, <https://doi.org/10.1093/bioinformatics/bts034>.
- [15] K. Yoshihara, M. Shahmoradgoli, E. Martínez, R. Vegesna, H. Kim, W. Torres-García, et al., Inferring tumour purity and stromal and immune cell admixture from expression data, *Nat. Commun.* 4 (2013) 2612, <https://doi.org/10.1038/ncomms3612>.
- [16] P. Charoentong, F. Finotello, M. Angelova, C. Mayer, M. Efremova, D. Rieder, et al., Pan-cancer immunogenomic analyses reveal genotype-immunophenotype relationships and predictors of response to checkpoint blockade, *Cell Rep.* 18 (1) (2017) 248–262, <https://doi.org/10.1016/j.celrep.2016.12.019>.
- [17] S. Du, Z. Yang, X. Lu, S. Yousuf, M. Zhao, W. Li, et al., Anoikis resistant gastric cancer cells promote angiogenesis and peritoneal metastasis through C/EBPβ-mediated PDGFB autocrine and paracrine signaling, *Oncogene* 40 (38) (2021) 5764–5779, <https://doi.org/10.1038/s41388-021-01988-y>.
- [18] Y. Yu, Y. Song, L. Cheng, L. Chen, B. Liu, D. Lu, et al., CircCEMIP promotes anoikis-resistance by enhancing protective autophagy in prostate cancer cells, *J. Exp. Clin. Cancer Res.* 41 (1) (2022) 188, <https://doi.org/10.1186/s13046-022-02381-7>.
- [19] Y.F. Tsai, C.C. Huang, Y.S. Lin, C.Y. Hsu, C.P. Huang, C.Y. Liu, et al., Interleukin 17A promotes cell migration, enhances anoikis resistance, and creates a microenvironment suitable for triple negative breast cancer tumor metastasis, *Cancer Immunol. Immunother.* 70 (8) (2021) 2339–2351, <https://doi.org/10.1007/s00262-021-02867-x>.
- [20] T. Zhang, B. Wang, F. Su, B. Gu, L. Xiang, L. Gao, et al., TCF7L2 promotes anoikis resistance and metastasis of gastric cancer by transcriptionally activating PLAU, *Int. J. Biol. Sci.* 18 (11) (2022) 4560–4577, <https://doi.org/10.7150/ijbs.69933>.
- [21] J. Song, Y. Liu, F. Liu, L. Zhang, G. Li, C. Yuan, et al., The 14-3-3σ protein promotes HCC anoikis resistance by inhibiting EGFR degradation and thereby activating the EGFR-dependent ERK1/2 signaling pathway, *Theranostics* 11 (3) (2021) 996–1015, <https://doi.org/10.7150/thno.51646>.
- [22] L. Yu, X. Wang, Y. Du, X. Zhang, Y. Ling, FASN knockdown inhibited anoikis resistance of gastric cancer cells via P-ERK1/2/Bcl-xL pathway, *Gastroenterol. Res. Pract.* 2021 (2021), 6674204, <https://doi.org/10.1155/2021/6674204>.

- [23] F.O. Adeshakin, A.O. Adeshakin, L.O. Afolabi, D. Yan, G. Zhang, X. Wan, Mechanisms for modulating anoikis resistance in cancer and the relevance of metabolic reprogramming, *Front. Oncol.* 11 (2021), 626577, <https://doi.org/10.3389/fonc.2021.626577>.
- [24] D.S. Chen, I. Mellman, Elements of cancer immunity and the cancer-immune set point, *Nature* 541 (7637) (2017) 321–330, <https://doi.org/10.1038/nature21349>.
- [25] J. Goc, C. Germain, T.K. Vo-Bourgeois, A. Lupo, C. Klein, S. Knockaert, et al., Dendritic cells in tumor-associated tertiary lymphoid structures signal a Th1 cytotoxic immune contexture and license the positive prognostic value of infiltrating CD8+ T cells, *Cancer Res.* 74 (3) (2014) 705–715, <https://doi.org/10.1158/0008-5472.Can-13-1342>.
- [26] J. Wang, R. Li, Y. Cao, Y. Gu, H. Fang, Y. Fei, et al., Intratumoral CXCR5(+)/CD8(+)/T associates with favorable clinical outcomes and immunogenic contexture in gastric cancer, *Nat. Commun.* 12 (1) (2021) 3080, <https://doi.org/10.1038/s41467-021-23356-w>.
- [27] I. Truxova, L. Kasikova, M. Hensler, P. Skapa, J. Laco, L. Pecen, et al., Mature dendritic cells correlate with favorable immune infiltrate and improved prognosis in ovarian carcinoma patients, *J. Immunother. Cancer* 6 (1) (2018) 139, <https://doi.org/10.1186/s40425-018-0446-3>.
- [28] A. Simiczyjew, E. Dratkiewicz, J. Mazurkiewicz, M. Ziętek, R. Matkowski, D. Nowak, The influence of tumor microenvironment on immune escape of melanoma, *Int. J. Mol. Sci.* 21 (21) (2020), <https://doi.org/10.3390/ijms21218359>.
- [29] M. Marzagalli, N.D. Ebel, E.R. Manuel, Unraveling the crosstalk between melanoma and immune cells in the tumor microenvironment, *Semin. Cancer Biol.* 59 (2019) 236–250, <https://doi.org/10.1016/j.semcancer.2019.08.002>.
- [30] F. Maibach, H. Sadozai, S.M. Seyed Jafari, R.E. Hunger, M. Schenk, Tumor-infiltrating lymphocytes and their prognostic value in cutaneous melanoma, *Front. Immunol.* 11 (2020) 2105, <https://doi.org/10.3389/fimmu.2020.02105>.
- [31] T. Nguyen, N. Kocovski, S. Macdonald, H.X.A. Yeang, M. Wang, P.J. Neeson, Multiplex immunohistochemistry analysis of melanoma tumor-infiltrating lymphocytes, *Methods Mol. Biol.* 2265 (2021) 557–572, https://doi.org/10.1007/978-1-0716-1205-7_39.
- [32] U. Dafni, O. Michielin, S.M. Lluesma, Z. Tsourti, V. Polydoropoulou, D. Karlis, et al., Efficacy of adoptive therapy with tumor-infiltrating lymphocytes and recombinant interleukin-2 in advanced cutaneous melanoma: a systematic review and meta-analysis, *Ann. Oncol.* 30 (12) (2019) 1902–1913, <https://doi.org/10.1093/annonc/mdz398>.
- [33] A.A. Sarnaik, O. Hamid, N.I. Khushalani, K.D. Lewis, T. Medina, H.M. Kluger, et al., Lifileucel, a tumor-infiltrating lymphocyte therapy, in metastatic melanoma, *J. Clin. Oncol.* 39 (24) (2021) 2656–2666, <https://doi.org/10.1200/jco.21.00612>.
- [34] J.H. van den Berg, B. Heemskerck, N. van Rooij, R. Gomez-Eerland, S. Michels, M. van Zon, et al., Tumor infiltrating lymphocytes (TIL) therapy in metastatic melanoma: boosting of neoantigen-specific T cell reactivity and long-term follow-up, *J. Immunother. Cancer* 8 (2) (2020), <https://doi.org/10.1136/jitc-2020-000848>.
- [35] A. Durgeau, Y. Virk, S. Corgnac, F. Mami-Chouaib, Recent advances in targeting CD8 T-cell immunity for more effective cancer immunotherapy, *Front. Immunol.* 9 (2018) 14, <https://doi.org/10.3389/fimmu.2018.00014>.
- [36] F. Piras, R. Colombari, L. Minerba, D. Murtas, C. Floris, C. Maxia, et al., The predictive value of CD8, CD4, CD68, and human leukocyte antigen-D-related cells in the prognosis of cutaneous malignant melanoma with vertical growth phase, *Cancer* 104 (6) (2005) 1246–1254, <https://doi.org/10.1002/cncr.21283>.
- [37] H. Kakavand, R.E. Vilain, J.S. Wilmott, H. Burke, J.H. Yearley, J.F. Thompson, et al., Tumor PD-L1 expression, immune cell correlates and PD-1+ lymphocytes in sentinel lymph node melanoma metastases, *Mod. Pathol.* 28 (12) (2015) 1535–1544, <https://doi.org/10.1038/modpathol.2015.110>.
- [38] K. Manabe, O. Yamasaki, Y. Nakagawa, T. Miyake, H. Udono, S. Morizane, Multifunctionality of CD8(+) T cells and PD-L1 expression as a biomarker of anti-PD-1 antibody efficacy in advanced melanoma, *J. Dermatol.* 48 (8) (2021) 1186–1192, <https://doi.org/10.1111/1346-8138.15904>.
- [39] M.S. Carlino, J. Larkin, G.V. Long, Immune checkpoint inhibitors in melanoma, *Lancet* 398 (10304) (2021) 1002–1014, [https://doi.org/10.1016/s0140-6736\(21\)01206-x](https://doi.org/10.1016/s0140-6736(21)01206-x).
- [40] B.P. Fairfax, C.A. Taylor, R.A. Watson, I. Nassiri, S. Danielli, H. Fang, et al., Peripheral CD8(+) T cell characteristics associated with durable responses to immune checkpoint blockade in patients with metastatic melanoma, *Nat. Med.* 26 (2) (2020) 193–199, <https://doi.org/10.1038/s41591-019-0734-6>.
- [41] R. Li, D. Han, J. Shi, Y. Han, P. Tan, R. Zhang, et al., Choosing tumor mutational burden wisely for immunotherapy: a hard road to explore, *Biochim. Biophys. Acta, Rev. Cancer* 1874 (2) (2020), 188420, <https://doi.org/10.1016/j.bbcan.2020.188420>.